Morphology of Polystyrene/Poly(methyl methacrylate) Blends: Effects of Carbon Nanotubes Aspect Ratio and Surface Modification

Jiaxi Guo, Nicholas Briggs, Steven Crossley, and Brian P. Grady
Carbon Nanotube Technology Center (CANTEC) and the School of Chemical, Biological and Materials Engineering, University of Oklahoma, Norman, OK 73019

DOI 10.1002/aic.14943
Published online July 16, 2015 in Wiley Online Library (wileyonlinelibrary.com)

Multiwalled carbon nanotubes (MWCNTs) with aspect ratios (ARs) ranging from 94 to 474 were incorporated into polystyrene (PS)/poly(methyl methacrylate) blends using solution mixing and melt mixing. Also, two functionalized MWCNTs were prepared from the nanotubes having AR 94: one was oxidized by nitric acid while the other was further modified with amine-terminated PS attached to carboxyl groups to form amides. The two functionalized MWCNTs (1 wt %) were used to show that which phase the carbon nanotubes (CNTs) were located in could be controlled with nanotube surface chemistry. When nanotubes were confined to the minor phase, the size of the minor domain first decreased with adding low AR CNT as expected due to the increased viscosity of the minor phase. However, at higher ARs, the size increased beyond the size for the minor domain with no nanotubes, and at high enough AR, the shape of the minor domain changed from spherical to an elongated irregular shape. © 2015 American Institute of Chemical Engineers *AIChE J*, 61: 3500–3510, 2015
Keywords: carbon nanotubes, aspect ratio, polymer blends, morphology, surface chemistry

Introduction

The morphology of immiscible polymer blends refers to the shape (continuous vs. sea-island; circle vs. irregular) and size of domains in the blends; the morphology has a great influence on blend properties.[1–13] The morphology can be tailored somewhat by polymer composition,[14–16] viscosity ratio,[14] annealing time/temperature,[8,9,14,17] flow rate of the blends,[6,14,18] interfacial forces between the polymers[14,19] as well as other factors. A third component acting as a modifier is often introduced to manipulate the morphology and/or the interfacial adhesion between the two immiscible components in order to improve blend performance. Fillers and especially nanofillers can change the morphology type and phase size mostly because of a combination of changed viscosity ratios during morphology creation and reduced coalescence due to steric hindrance. Examples of such fillers include nanoclay,[2–5,10,20] carbon black,[8,21] copolymers,[9,22–24] and nanoparticles.[11–13,25–27] For example, Filippone et al.[2] have incorporated organoclay into poly(ethylene)/poly (amide) 6 (PA6) blends and found that the clay changes the sea-island structure of the blends to the cocontinuous morphology, and the rubbery modulus of the composites increased. Carbon black[2] and nanoparticles[13] have also been found to change blend morphology. Copolymers[9,22–24] and Janus particles[25] can be located at the interface, and can reduce the domain size of the minor polymer phase as well as possibly increasing the interfacial adhesion.

Due to their excellent mechanical properties as well as high electrical and thermal conductivities, carbon nanotubes (CNTs) have been widely investigated in the field of material science and engineering.[28–36] For polymer blends, CNTs have been widely studied with respect to their location in the blends as well as their effect on the domain size and shape.[35–49] Zhang et al.[35] added pristine CNTs to polypropylene (PP)/PA6 blends, and found that the nanotubes were selectively located in the PA6 phase and formed an elongated structure that improved the electrical properties. Wu et al.[36] modified CNTs with maleic anhydride and added them into polystyrene (PS)/PP blends, and found that the modified CNTs act as a plasticizer for both polymers and as heterogeneous nucleating agents for PP. Several studies also indicated that the amount of CNTs also play a key role in the morphology change of the polymer blends.[38,39,41,49] In terms of the localization of the CNTs in the polymer blends, CNTs generally prefer to locate in one phase of a blend[35–48] and usually not at the interface or in both phases. Which phase seems to depend on the respective surface energies of the blend components, and the anisotropy of nanotubes is the reason for the very strong partitioning.[49]

In this work, we studied the effects of nanotube aspect ratio (AR) on blend morphology and nanotube surface chemistry on the location of CNTs in polymer blends. Blends of two immiscible amorphous polymers, PS and poly(methyl methacrylate) (PMMA), were studied in order to eliminate crystallinity effects. Any study of blends with one or both components being semicrystalline has the confounding effect of nucleation

Additional Supporting Information may be found in the online version of this article.

This contribution was identified by Da Deng (Wayne State University) as the Best Presentation in the session "Processing of Nanocomposites" of the 2013 AIChE Annual Meeting in San Francisco, CA

Correspondence concerning this article should be addressed to B. P. Grady at bpgrady@ou.edu

Table 1. MWCNT Average Length and Diameters

CNTs	Diameter[a] (nm)	Initial length[b] (μm)	Initial length (μm)	Length after melt mixing (μm)
AR 94	7.8	0.74	0.95	0.84
AR 250	10.4	2.60	n/a	2.32
AR 313	9.9	3.10	n/a	2.96
AR474	9.5	4.50	4.23	4.12

[a]Measured with TEM.[51]
[b]Measured with AFM.[51]

by nanotubes prohibiting the isolation of the effect of nanotubes on blend morphology. For AR studies, multiwalled carbon nanotubes (MWCNTs) having different ARs ranging from 94 to 474 were investigated; no other studies to our knowledge have examined the effect of nanotube AR on blend morphology. In fact, most commercial MWCNTs have an AR around 100.[50] Both melt mixing and solution mixing were carried out to prepare nanotube/polymer blend composites. Solution mixing has the advantage of creating a morphology that is not as affected by kinetic factors with slow solvent evaporation and thermal annealing. Melt mixing has the advantage of eliminating the influence of the interactions between solvent and CNTs. In other words, the fact that one type of nanotube might tend to agglomerate in the solvent vs. another is not an issue in melt mixing. For nanotube chemistry studies, three types of AR 94 nanotubes, pristine (untreated), nitric acid treated, and PS-grafted after nitric acid treatment, were melt mixed with PS/PMMA blends.

Experimental

Materials

PS having average $M_w \sim 210$ kg/mol was from Dow Chemical and the PMMA, having average $M_w \sim 120$ kg/mol was from Sigma Aldrich. Four different MWCNTs (SouthWest Nanotechnologies, Norman, OK) were investigated, where the diameter, length, and the AR for each MWCNT are shown in Table 1. The average ARs are 94, 250, 313, and 474, respectively, with CNT lengths ranging from 0.95 to 4.23 μm and diameters at $\sim$10 nm and the number of concentric cylinders was roughly identical as well. All tubes were made using the same general procedure; with AR 94 being commercially available as SWeNT® SMW100 and AR 474 being available as SWeNT® SMW200. Analyses for the length and diameter of pristine CNTs were described elsewhere.[51]

Chemical modification of nanotubes

AR 94 tubes were oxidized using a solution of 35% nitric acid (Sigma Aldrich) following the method described in the literature.[52] The CNT and nitric acid mixture was first bath sonicated at 45°C for 30 min, followed by vacuum-filtering using a Teflon membrane with pore size 0.2 μ (PTFE 0.2 μ). The black solid was then rinsed with deionized water until the rinsed water had a pH = 7. The resultant black samples were dried at 80°C overnight under vacuum. Acid-functionalized AR 94 is labeled as AF-MWCNTs.

A portion of the AF-MWCNTs were then dispersed in thionyl chloride ($SOCl_2$) to convert the —COOH groups to —COCl groups on the surface of the MWCNTs. Typically, 100 mg of the AF-MWCNTs were dispersed in 20 mL $SOCl_2$ followed by magnetic stirring at 70°C for 24 h. The resultant mixture was then centrifuged at 3000 rpm for 10 min. The supernatant of the mixture was carefully removed. The black solid obtained was dispersed in 10-mL dimethylformamide (DMF) along with 500 mg amine-terminated polystyrene (NH_2-PS, M_w =108 kg/mol and polydispersity index (PDI) = 1.12, from Polymer Science). The mixture was bubbled with nitrogen and bath sonicated for 30 min. Samples were transferred to a hotplate with stirring at 130°C for 4 days under nitrogen atmosphere. After reaction, the samples were rinsed with DMF to remove unreacted NH_2-PS. The black solid was finally dried at 80°C overnight under vacuum. The samples obtained are MWCNTs grafted with PS are labeled as PS-MWCNTs. PS-MWCNTs were investigated by transmission electron microscopy (TEM) and the images are shown on the right hand side of Figure 1a, where amorphous formations are observed to coat on the CNTs as indicated by the arrows, indicating that the PS has been successfully coated on the CNTs. In addition, thermogravimetric analysis shows that approximately 30 wt % PS was grafted on the surface of the CNTs as indicated in Figure 1b (gas conditions: mixture of helium and air at flow rate of 10 and 40 mL min^{-1}).

Composites preparation

For solution mixing, PS/PMMA blends mixed with pristine MWCNTs having different ARs ranging from 94 to 474 were prepared in toluene (Sigma Aldrich). MWCNTs of 0.4 mg weight were first dispersed in 5 mL toluene using bath sonication for 20 min; bath sonication was used instead of horn sonication because the bath sonication intensity was much weaker (i.e., to lessen nanotube breakage). Twenty minutes was chosen because this time was found to be the minimum required so that no nanotubes were observed on the bottom of the vial in 1 h, which we assumed was a measure of good dispersion. In a separate glass vial, 40 mg PS-90K/PMMA blends were dissolved in 5 mL toluene, and the PS-90K/PMMA solution was then mixed with the nanotubes, further bath sonicated for 30 min to assure good dispersion of MWCNTs in the polymer blends. The samples prepared by this method are shown in Table 2, where the components of each of the samples are listed.

For melt mixing, composites were prepared using a DSM twin-screw micro compounder having volume 5 cm^3 (DSM Xplore, MD Geleen, The Netherlands). Before mixing, the samples were dried at 80°C under vacuum overnight. CNTs weighing 0.04 g (either pristine or modified) were premixed with 4 g of PS/PMMA blends in a glass vial. The mixtures were then fed into the compounder with mixing conditions: 5 min at 190°C and a mixing speed of 150 rpm under nitrogen atmosphere, and the extruded strands were used as described below. Samples prepared by this method are also shown in Table 2. This article mostly focuses on blends in which the ratio of PS:PMMA is 80:20 in weight, and hence, PMMA is a minor phase due to the fact that the CNTs, except for those coated with PS, are found in the PMMA domain as will be shown later.

Morphology characterization

Scanning electron microscopy (SEM) was applied to characterize the domain size of the samples on a Zeiss NEON High Resolution SEM and a ZEISS DSM-960A SEM. For solution-mixed samples, several drops of the mixture were placed on a silicon substrate, and the samples were placed in the fume hood until the solvent evaporated. The thin film obtained was annealed in a vacuum oven at 170°C for 5 h to ensure the surface concentration ratio of PS/PMMA film is stable at the original

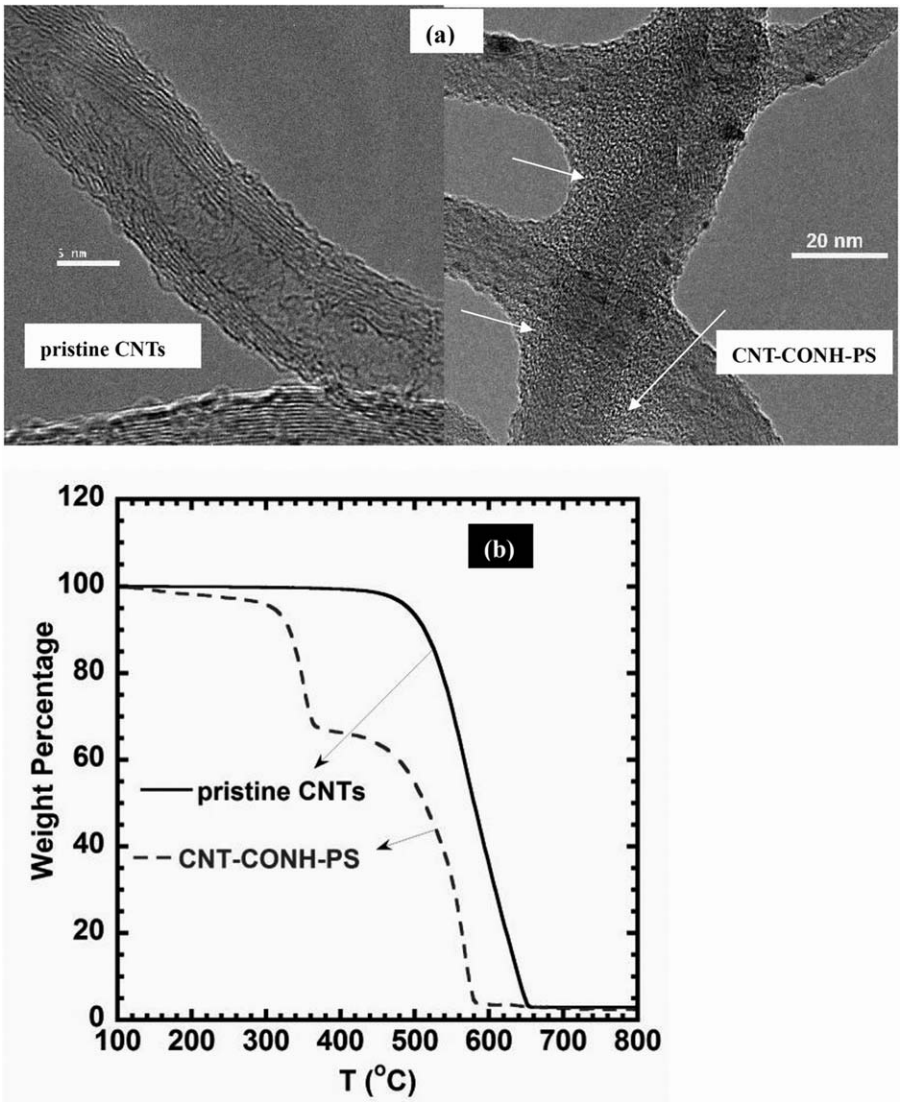

Figure 1. Transmission electron microscopy images (a) and thermogravimetric analysis (b) for the pristine AR 94 carbon nanotubes and the carbon nanotubes grafted with polystyrene.

The arrows in (a) indicate amorphous PS formations on the surface of the carbon nanotubes.

mixing ratio.[53] After cooling to room temperature, the samples were submerged in formic acid to remove the PMMA phase (or the cyclohexane to remove the PS domain), following by rinsing with formic acid (or cyclohexane), and then drying in the oven at 80°C for overnight. For melt-mixed samples, the extruded strands were cryogenically fractured in liquid nitrogen and the

Table 2. Components of the PS/PMMA/CNTs Composites Prepared via Solution and Melt Mixings*

	Samples	PS/PMMA	CNTs	SF	D_n (μm)	D_v (μm)
Solution mixing	S-0	80/20	n/a	1.00	1.07	1.73
	S-1	80/20	AR 94	0.79	0.66	1.35
	S-2	80/20	AR 250	0.74	1.18	1.77
	S-3	80/20	AR 313	0.70	1.38	2.19
	S-4	80/20	AR474	0.65	1.45	2.18
Melt mixing	M-0	80/20	n/a	0.91	0.75	1.03
	M-1	80/20	AR 94	0.89	0.64	0.92
	M-2	80/20	AR 250	0.86	0.78	0.99
	M-3	80/20	AR 313	0.78	0.92	1.46
	M-4	80/20	AR474	0.77	1.16	1.55
	M-5	20/80	AR 94	n/a	n/a	n/a
	M-6	80/20	AR 94 acid functionalized	n/a	n/a	n/a
	M-7	20/80	AR 94 acid functionalized	n/a	n/a	n/a
	M-8	20/80	AR 94 polystyrene grafted	n/a	n/a	n/a
	M-9	80/20	AR 94 polystyrene grafted	n/a	n/a	n/a

*In all cases, the amount of CNTs is 1 wt % in the composites. SF, D_n, and D_v are defined in Eqs. 1, 2, and 3, respectively.

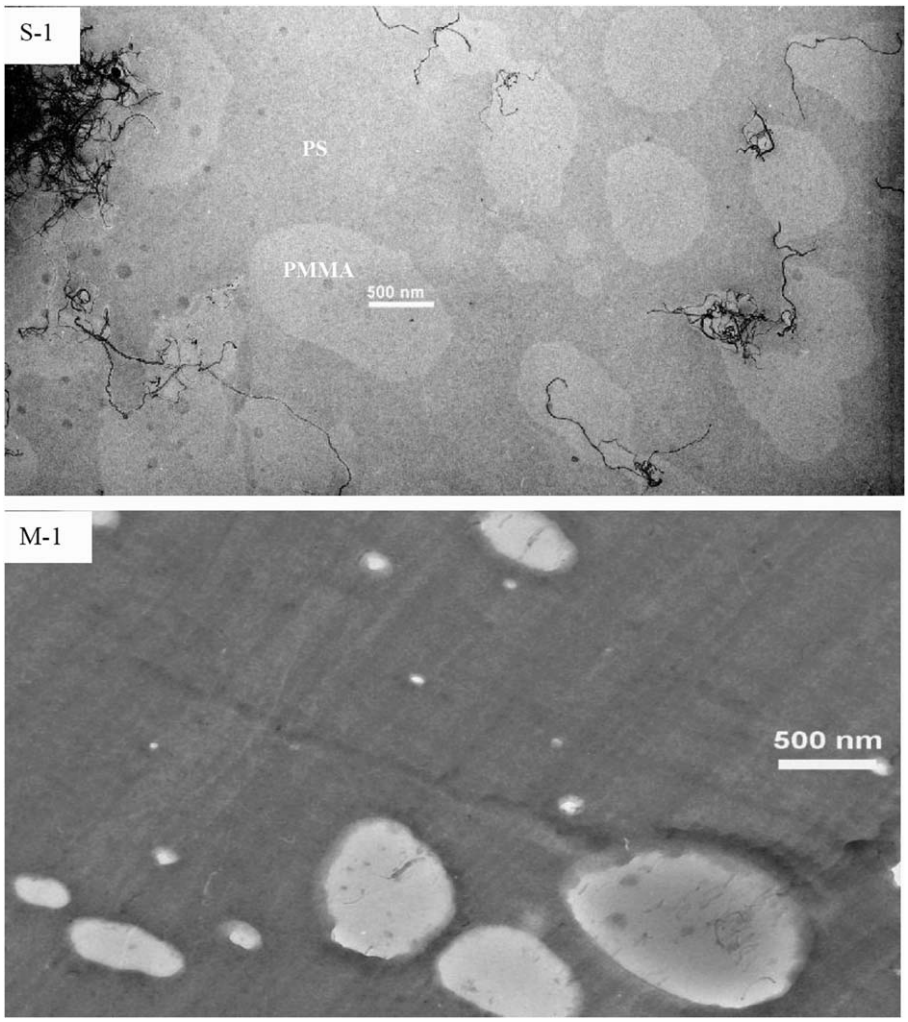

Figure 2. TEM images for the solution-mixed and melt-mixed samples having CNTs with aspect ratios 94.

The less dark phase is PMMA and the dark phase is PS domain.

fractured samples were placed in formic acid to extract the PMMA domain (or in cyclohexane to extract the PS domain). The samples were then rinsed with formic acid (or cyclohexane), and finally dried in a vacuum oven at 80°C overnight. Before the SEM experiment, samples were coated with approximately a 4-nm-thick layer of iridium to enhance visibility.

TEM experiments were carried out with a JEOL 2000-FX TEM using an accelerating voltage of 200kV. The samples prepared by solution mixing were spin-coated to form a thin film and then annealed at the same conditions as the SEM samples. For the melt-mixing samples, the extruded strand was sectioned by a microtome to obtain thin films having thickness approximately 100 nm, and the thin films were collected using the lacey carbon substrate. All TEM samples were stained by ruthenium tetroxide (RuO_4) to obtain good contrast between the PS and PMMA domains. Because RuO_4 will stain the aromatic groups on the PS, the PS phase will present as the darker phase on the TEM image.[54]

Shape and domain size determination

The morphology of the PS/PMMA blends was characterized with respect to both shape and size from micrographs based on more than 200 domains. The shape factor (SF) was used to characterize the shape of the blends and it was calculated by the equation shown below[55]

$$SF = \frac{\sum A_i \frac{4\pi A_i}{P_i^2}}{\sum A_i} \tag{1}$$

where A_i and P_i are the area and perimeter of the minor-phase domain. The value for SF ranges from 0 to 1, indicating the shapes from line to circle. The size of the minor polymer phase was characterized by the number average diameter (D_n) and volume average diameter (D_v) determined following the method proposed in the literature[56] as shown below

$$D_n = \frac{\sum N_i D_i}{\sum N_i} \tag{2}$$

$$D_v = \frac{\sum N_i D_i^3}{\sum N_i D_i^2} \tag{3}$$

where N_i and D_i are the number and diameter of the ith domain, respectively. For Eqs. 2 and 3 where the domains were not circular in the two-dimensional (2-D) image, the average diameter was used.

Length measurements

The length of CNTs with different AR after melt mixing was determined by SEM. To measure the CNTs lengths after melt mixing, a procedure similar to Krause et al.[57] was used.

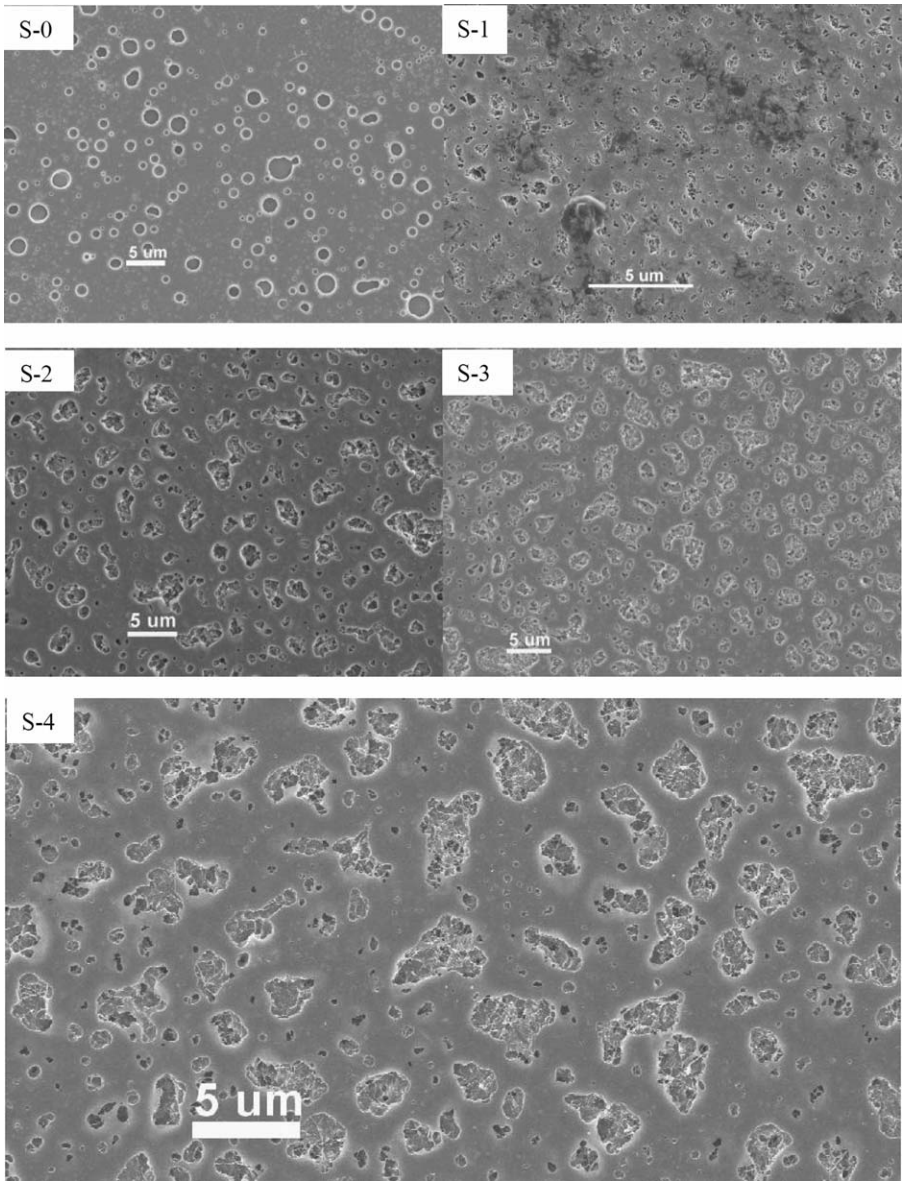

Figure 3. SEM images for the PS/PMMA/CNTs composites prepared via solution mixing where CNTs have aspect ratio ranging from 94 to 474 as indicated in Table 2.

The ratio of PMMA:PS is 20:80 and the PMMA domain has been extracted by formic acid.

First, 100 mg of the polymer blend was loaded in a vial of 20 mL of DMF. The vial was heated at 60°C and mixed with a magnetic stir bar to dissolve the polymer. The solution was then filtered with a 0.22 μm PTFE filter to isolate the nanotubes. While the CNTs were still on the filter an additional 200 mL of DMF was used to rinse the CNTs and remove any residual polymer. The filter was then placed in 50 mL of DMF and bath sonicated for 30 s. This step was done to dislodge the CNTs from the filter. On a silicon wafer, 0.25 mL of the DMF solution with the CNTs was deposited on a 2×2 cm^2 Si wafer and allowed to dry overnight in a fume hood. For as-received nanotubes, $\sim$3 mg of CNTs were dispersed in 20 mL of DMF using bath sonication for 30 min, followed by depositing a 0.25 mL drop on the a 2×2 cm^2 Si wafer and drying overnight in the fume hood. To measure the length of the CNTs, a Zeis Neon 40EsB SEM was used and the average contour length for each nanotube sample was calculated based on the results of 100 tubes.

Results and Discussion

The location of the pristine CNTs with AR 94 in the PS/PMMA blends are shown in Figure 2 for the samples prepared by solution and melt mixing, respectively, where the images were taken by TEM with PMMA as the minor domain (for comparison, a TEM image with PMMA as the major domain prepared via melt mixing is shown in Figure 6). In Figure 2, the PS is the main phase (80 wt %), which is shown in dark. As shown in the figure, the CNTs primarily locate in the PMMA phase for the samples prepared by both solution and melt mixing (similar results are shown in Figure 6), in agreement with the literature that CNTs prefer to stay or migrate to a more polar domain in polymer blends.[35,38,41–46] In addition, for all nanotubes with different AR, SEM images (shown in Figures 3 and 4, Supporting Information, Figures S-1, and S-2) demonstrate that after the PMMA phase was extracted, the nanotubes locate in the holes (PMMA), while after the PS phase was extracted, the nanotubes locate on the surface of the

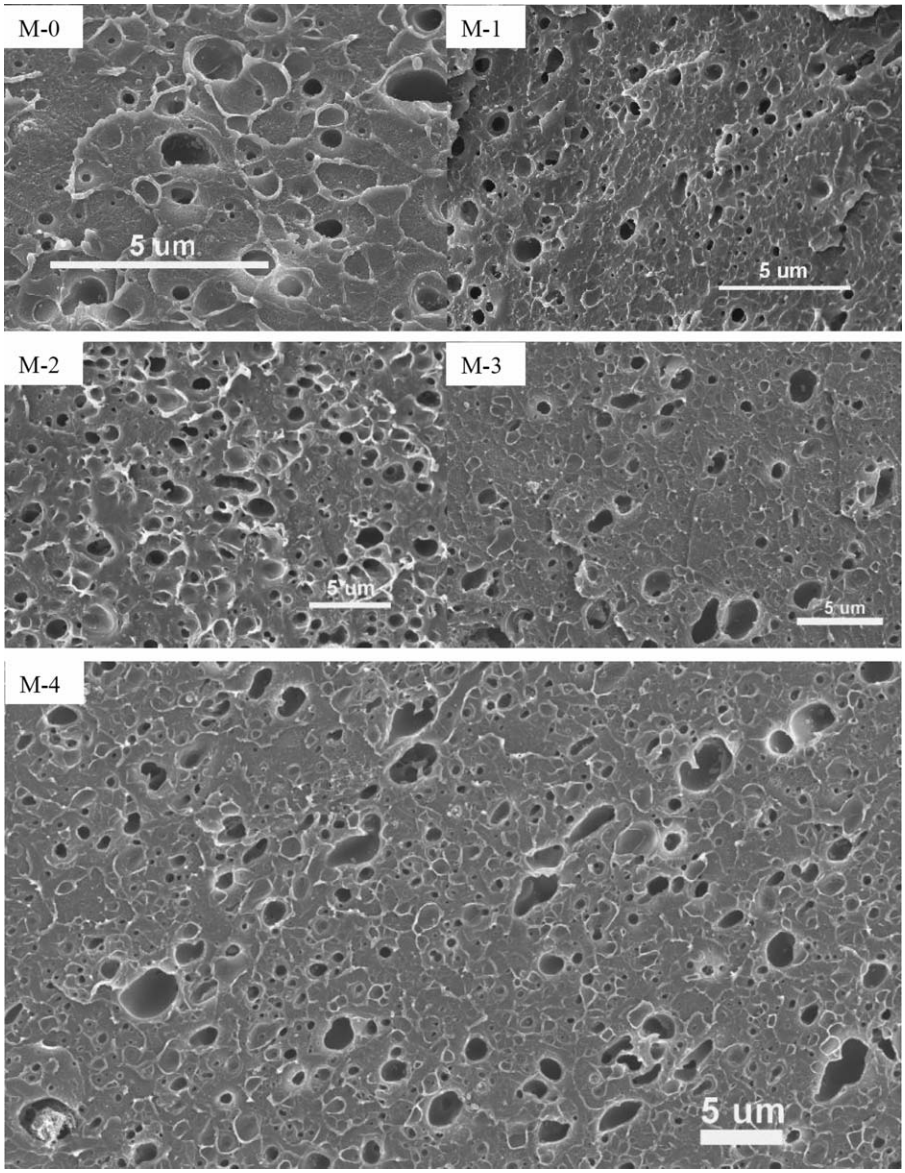

Figure 4. SEM images for the PS/PMMA/CNTs composites prepared via melt mixing where CNTs have aspect ratio ranging from 94 to 474 as indicated in Table 2.

The ratio of PMMA:PS is 20:80 and the PMMA domain has been extracted by formic acid.

PMMA, further indicating that the MWCNTs prefer to stay in the PMMA domain. Therefore, this article will focus on how the nanotubes change the PMMA morphology in the PMMA/PS blends, where the PMMA is the minor phase in the blends.

Figure 3 shows SEM images for the PS/PMMA blends mixed with and without nanotubes via solution mixing. SEM was used to characterize the shape and size of the PMMA domain, instead of TEM, due to the fact that the latter may have overlapped domains. By inspection of Figure 3, the SF and domain size of the polymer blends are influenced by changing the AR of the MWCNTs. To quantitatively analyze the effects of the AR on the shape and size of the polymer blends, values for the PMMA minor phase based on Eqs. 1–3 are shown in Table 2. As demonstrated in Table 2, for solution mixing, the SF of PMMA in the neat PS/PMMA blends is 1.00, but reduces with increasing AR of the nanotubes. However, even more dramatic than the SF change is how the morphology becomes much more irregular with AR as shown in Figure 3.

Figure 4 shows SEM images for the PS/PMMA blends mixed with and without nanotubes via melt mixing and the PMMA phase was extracted by formic acid. The SF for the PMMA phase shows less reduction upon adding nanotubes for samples made by melt mixing vs. those made by solution mixing consistent with a visual comparison between Figures 3 and 4. Our initial hypothesis was that the length reduction of the nanotubes in the melt was much greater than that in solution, which caused the smaller effect; however, length reduction after processing was minimal as shown in Table 1 and Figure 5. In fact, the results in Table 1 concerning length reduction via melt mixing in a conical twin-screw stand in stark contrast to those presented elsewhere in which the length reduction was significant after melt mixing for MWCNTs with AR $\sim$100[57–61] and even more significant with higher AR tubes.[51] We do not observe great breakage of nanotubes in this work presumably due to the protection from the capsule effects of the minor phase in the polymer blends (a detailed investigation on the breakage CNTs in melt mixing of polymer blends will

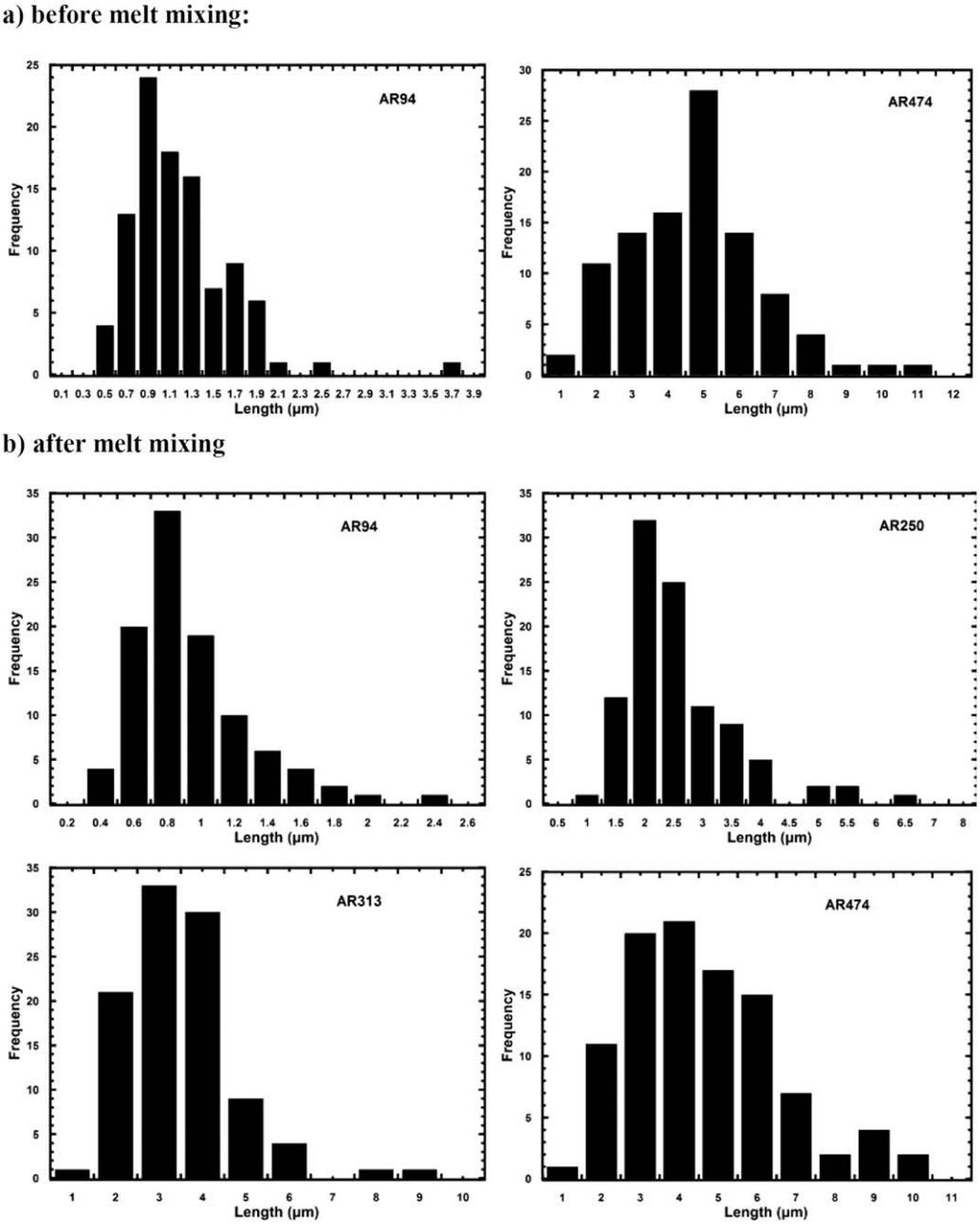

Figure 5. Length distribution for the CNTs with aspect ratios ranging from 94 to 474 before (a) and after (b) melt mixing.

be the subject of a future study). Overall, perhaps the reason for the smaller changes in anisotropy shown in melt mixing is that the films prepared by solution mixing are more 2-D, while that in the samples prepared by melt mixing are more 3-D; such a difference in dimensionality would be expected cause such difference in SF response for 2-D images. Regardless, samples prepared by both methods indicate that the PMMA phase became more anisotropic when adding CNTs in the blends.

The number average diameter (D_n) and volume average diameter (D_v) of the PMMA domain first decreases with adding the shorter nanotubes (AR 94), but then increases with increasing length of the CNTs. For solution mixing, the D_n decreases from 1.07 μm for the neat polymer blends to 0.66 μm and D_v reduces from 1.73 to 1.35 μm when adding 1 wt % AR 94 nanotubes. When adding longer nanotubes, D_n and D_v both increase with increasing the length of CNTs. For example, with AR 250 (length $\sim$ 2.6 μm) and AR 474 (length $\sim$ 4.23 μm) CNTs, D_n of PMMA phase is 1.18 and 1.45 μm, respectively, both higher than the counterpart in the neat PS/PMMA blends. For melt mixing, very similar behavior has been observed that D_n and D_v first decrease with adding short nanotubes, and then both increase with increasing the AR (length) of CNTs.

The average diameters are clearly much smaller than the nanotube lengths. However, what about the maximum dimension of the nanotubes, is it reasonable that the nanotubes will fit inside of the domains? For the AR 94 tubes (length $\sim$ 0.9 μm), the maximum length of the domain is less than the average length of the nanotubes. For the remainder of the tubes, the maximum lengths of the domain shown in Figures 3 and 4 seem to be long enough that tubes of these contour lengths

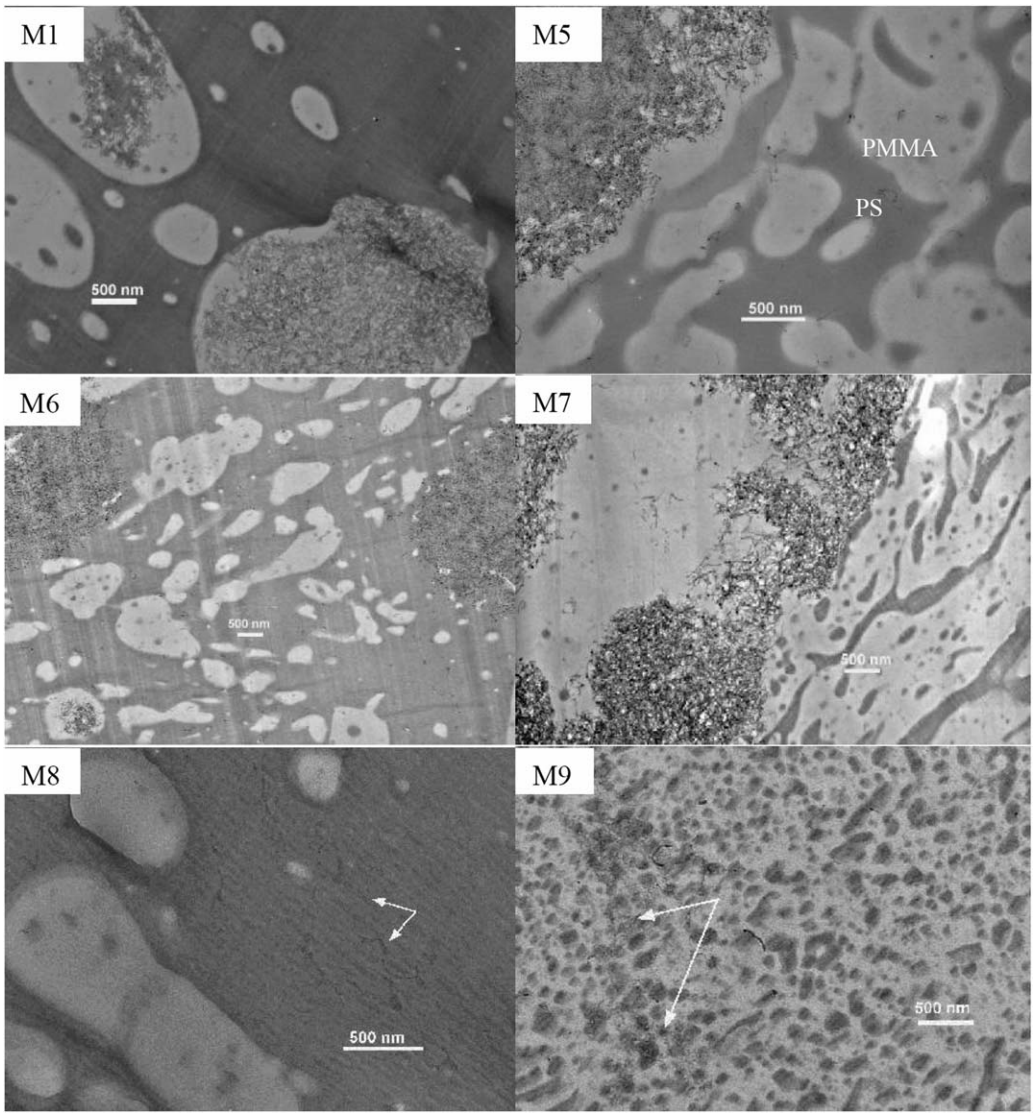

Figure 6. TEM results for the polymer blends incorporated with pristine, acid oxidated, and PS-grafted carbon nanotubes using melt mixing.

The components of each sample are indicated in Table 2. The arrows in M5 and M6 indicate carbon nanotubes. The less dark phase is PMMA and the dark phase is PS domain.

could be encapsulated within, given that MWCNTs are definitely not straight as Figure 2 shows. We do not understand why the domains for the AR 94 tubes do not encapsulate the tubes.

Hence, at lengths typical of most commercial nanotubes, nanotubes located in the dispersed phase reduce the dispersed phase size substantially likely due to the significant increase in minor phase viscosity that occurs with the addition of nanotubes, hindering drop coalescence. CNTs have been found[38,39,41] to influence the domain size of the polymer blends previously as a function of nanotube composition, but this report is the first time to our knowledge that the AR of CNTs is found to also influence the shape of the minor phase for blends of two amorphous polymers. Obviously, the large nanotube persistence and contour lengths force a distortion of the normal spherical shape so as to encapsulate the highly anisotropic nanotubes. Further, with increasing length of CNTs, the domain size of the minor phase that contains the nanotubes increases as well. Single-walled CNTs can be forced to bend to form a ring in oil/water or water/oil emulsion and the size of the ring depends on the size of the droplet.[34] In our case with MWCNTs, the polymer droplet changes shape and size to include the nanotubes in the PMMA domain as shown in Figures 3 and 4. These two situations represent opposite ends of possible behavior, in one case, the forces are large enough and the flexural rigidity small enough to cause the long anisotropic nanotube to bend, while in the other case, the phase reshapes itself to encapsulate the filler.

In the case of the PS/PMMA blends (20/80 in weight) where PMMA is the main phase, no results for the domain size are available for the composites due to the fact that the CNTs prefer to locate in the PMMA domain (Figures 2 and 6) and the morphology of the polymer blends without and with CNTs are found to exhibit cocontinuous structure (shown in Figure 6 and Supporting Information, Figures S-1 and S-2). The addition of longer nanotubes does seem to alter the morphology, but clear trends cannot be established based on the EM images collected.

The location of the CNTs in the PS/PMMA polymer blends was investigated on the AR 94 nanotubes having different

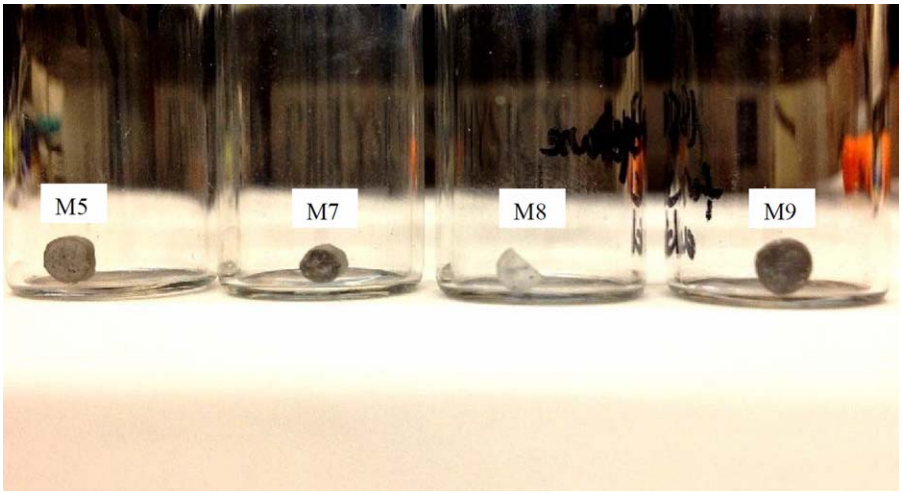

Figure 7. Comparisons among the PS/PMMA blends with different carbon nanotubes after extraction experiment in the solvent: M5, M7, and M9 were submerged in the cyclohexane to extract the PS phase (20 wt %); M8 was submerged in the formic acid to extract the PMMA domain (20 wt %)

[Color figure can be viewed in the online issue, which is available at wileyonlinelibrary.com.]

functionalities: pristine, acid-functionalized, and PS-grafted CNTs. The three types of CNTs were melt mixed with the PS/PMMA blends at the mass ratio of either 80/20 or 20/80 as indicated in Table 2. The samples obtained were microtomed into thin films and observed with TEM, and the results are shown in Figure 6. For both pristine samples M1 and M5, most of the CNTs locate in the PMMA domain, independent of the amount of the PMMA, which was also shown Figure 2. In samples M6 and M7, where the CNTs have been oxidized by nitric acid to produce carboxylic groups on the surface, CNTs also locate in the PMMA domain, regardless of the size of the PMMA phase. Finally, for M8 and M9, where CNTs were grafted with PS on the surface, the nanotubes are found primarily in the PS domain. To further investigate localization of the nanotubes, samples M5, M7, and M8 having 20 wt % PS were submerged in the cyclohexane to selectively extract the PS domain; also, the sample M9 having 20 wt % PMMA and 1 wt % PS-grafted CNTs was submerged in the formic acid to remove the PMMA domain. The composites after selective extraction are shown in Figure 7. Sample M8 is much lighter than the rest of the samples shown in the same picture: M8 is nearly white, whereas the other three samples are still black demonstrating that the PS-MWCNTs locate in the PS domain because the nanotubes are able to be extracted using a solvent for the PS only.

This finding for PS/PMMA blends is in good agreement with several studies that different functionalities on their surface can either yield different localizations for the CNTs in other polymer blends,[62–65] or selectively insert in the hard phase or the soft phase in a polyurethane.[66] The localization adjustments for CNTs in the polymer blends confirms that different functional groups on the surface of CNTs can drive the nanotubes to be found in a different phase.

Conclusion

The morphology of the PS and PMMA polymer blends has been altered using CNTs having different ARs ranging from 94 to 474 and different surface functional groups. The former changes both the shape and domain size when the nanotubes partition into the minor phase, while the effect of the latter is with respect to which phase the nanotubes will partition. The SF was found to decrease with adding CNTs, indicating the minor domain becomes much less circular, and also decrease with an increase in AR (or length) at the same added tube fraction. In addition, the domain size of the minor phase has been found to decrease significantly when adding CNTs with AR 94 due to the higher viscosity of the minor phase that inhibits drop coalescence. The domain size increases with increasing ARs when adding nanotubes with ARs ranging from 250 to 474 becoming substantially larger than the domain size with no nanotube addition due to the fact that for the minor phase to encapsulate these long tubes, the domain size must get larger.

We have also shown that the preferred phase for a nanotube can be altered based on the surface chemistry of the nanotube. Along with viscosity, which is a well-known way to alter blend morphology, this work has shown that the morphology of polymer blends can be altered substantially by changing the length of a high AR nanofiller as well as changing surface chemistry.

Acknowledgments

The authors greatly acknowledge the help from Preston Larson and Gregory Strout for the SEM and TEM measurements. The authors would also like to thank Southwest Nanotechnologies for supplying the nanotubes used in this study and many discussions over the years.

Literature Cited

1. Utracki L. *Polymer Blends Handbook*. Dodrecht: Kluwer Academic Publishers, 2002.
2. Filippone G, Dintcheva NT, Acierno D, La Mantia FP, Using organoclay to promote morphology refinement and co-continuity in high-density polyethylene/polyamide 6 blends – effect of filler content and polymer matrix composition. Polymer. 2008;49:1312–1322.
3. Lee MH, Dan CH, Kim JH, Cha J, Kim S, Hwang Y, Lee CH. Effect of clay on the morphology and properties of PMMA/poly (styrene-co-acrylonitrile)/clay nanocomposites prepared by melt mixing. *Polymer*. 2006;47: 4359–4369.
4. Ray SS, Bousmina M, Maazouz A. Morphology and properties of organoclay modified polycarbonate/poly (methyl methacrylate) blend. *Polym Eng Sci*. 2006;46:1121–1129.

5. Khatua BB, Lee DJ, Kim HY, Kim JK. Effect of organoclay platelets on morphology of nylon-6 and poly (ethylene-r an-propylene) rubber blends. *Macromolecules*. 2004;37:2454–2459.
6. Zhang ZL, Zhang HD, Yang YL, Vinckier I, Laun HM. Rheology and morphology of phase-separating polymer blends. *Macromolecules*. 2001;34:1416–1429.
7. Knackstedt MA, Roberts AP. Morphology and macroscopic properties of conducting polymer blends. *Macromolecules*. 1996;29: 1369–1371.
8. Gubbels F, Blacher S, Vanlathem E, Jerome R, Deltour R, Brouers F, Teyssie Ph. Design of electrical composites: determining the role of the morphology on the electrical properties of carbon black filled polymer blends. *Macromolecules*. 1995;28:1559–1566.
9. Kim JK, Zhou HY, Nguyen SBT, Torkelson JM. Synthesis and application of styrene/4-hydroxystyrene gradient copolymers made by controlled radical polymerization: compatibilization of immiscible polymer blends via hydrogen-bonding effects. *Polymer*. 2006;47: 5799–5809.
10. Gelfer MY, Song HH, Liu LZ, Hsiao BS, Chu BJ, Rafailovich M, Si MY, Zaitsev VJ. Effects of organoclays on morphology and thermal and rheological properties of polystyrene and poly (methyl methacrylate) blends. *Polym Sci B: Polym Phys*. 2003;41:44–54.
11. Zhang WH, Fu BX, Seo Y, Schrag E, Hsiao B, Mather PT, Yang NL, Xu DY, Ade H, Rafailovich M, Sokolov J. Effect of methyl methacrylate/polyhedral oligomeric silsesquioxane random copolymers in compatibilization of polystyrene and poly(methyl methacrylate) blends. *Macromolecules*. 2002;35:8029–8038.
12. Cai XX, Li BP, Pan L, Wu GZ. Morphology evolution of immiscible polymer blends as directed by nanoparticle self-agglomeration. *Polymer*. 2012;53:259–266.
13. Elias L, Fenouillot F, Majeste JC, Cassagnau Ph. Morphology and rheology of immiscible polymer blends filled with silica nanoparticles. *Polymer*. 2007;48:6029–6040.
14. Utracki LA, Shi ZH. Development of polymer blend morphology during compounding in a twin-screw extruder. Part I: droplet dispersion and coalescence—a review. *Polym Eng Sci*. 1992;32: 1824–1833.
15. Min K, White JL, Fellers JF. Development of phase morphology in incompatible polymer blends during mixing and its variation in extrusion. *Polym Eng Sci*. 1984;24:1327–1336.
16. Schmitt RL, Gardella JA, Jr, Salvati L, Jr. Studies of surface composition and morphology in polymers. 2. Bisphenol A polycarbonate and poly (dimethylsiloxane) blends. *Macromolecules*. 1986;19:648–651.
17. Xie XM, Chen Y, Zhang ZM, Tanioka A, Matsuoka M, Takemura K. Controls of gradient morphology and surface properties of polymer blends. *Macromolecules*. 1999;32:4424–4429.
18. Kim JR, Jamieson AM, Hudson SD, Manas-Zloczower I, Ishida H. Influence of exothermic interaction on the morphology and droplet coalescence of melt-mixed immiscible polymer blends containing a block copolymer. *Macromolecules*. 1998;31:5383–5390.
19. Hobbs SY, Dekkers MEJ, Watkins VH. Effect of interfacial forces on polymer blend morphologies. *Polymer*. 1988; 29:1598–1602.
20. Wang Y, Zhang Q, Fu Q. Compatibilization of immiscible poly (propylene)/polystyrene blends using clay. *Macromol Rapid Commun*. 2003;24:231–235.
21. Huang JC. Carbon black filled conducting polymers and polymer blends. *Adv Polym Technol*. 2002;21:299–313.
22. Fayt R, Jerome R, Teyssie P. Molecular design of multicomponent polymer systems, 13. Control of the morphology of polyethylene/ polystyrene blends by block copolymers. *Makromol Chem*. 1986; 187:837–852.
23. Pu GW, Luo YW, Wang AN, Li BG. Tuning polymer blends to cocontinuous morphology by asymmetric diblock copolymers as the surfactants. *Macromolecules*. 2011;44:2934–2943.
24. Robeson LM. *Polymer Blends: A Comprehensive Review*.Germany: Hanser Publications, 2007.
25. Walther A, Matussek K, Muller AHE. Engineering nanostructured polymer blends with controlled nanoparticle location using Janus particles. *ACS Nano*. 2008;2:1167–1178.
26. Bandyopadhyay D, Douglas JF, Karim A. Influence of C60 nanoparticles on the stability and morphology of miscible polymer blend films. *Macromolecules*. 2011;44:8136–8142.
27. Fenouillot F, Cassagnau P, Majeste JC. Uneven distribution of nanoparticles in immiscible fluids: morphology development in polymer blends. *Polymer*. 2009;50:1333–1350.
28. Grady BP. *Carbon Nanotube-Polymer Composites: Manufacture, Properties, and Applications*. New York: Wiley, 2011.
29. Rui Y, Guo JX, Harwell J, Nakanishi T, Kotera S, Grady GP. Electrical, mechanical, and crystallization properties of ethylene-tetrafluoroethylene copolymer/multiwalled carbon nanotube composites. *J Appl Polym Sci*. 2014;131:41052.
30. Ling YF, Gu G, Liu RY, Lu XJ, Kayastha V, Jones CS, Shih WS, Janzen DC, Investigation of the humidity-dependent conductance of single-walled carbon nanotube networks. *J Appl Phys*. 2013;113: 024312.
31. Guo JX, Saha P, Liang JF, Saha M, Grady GP. Multi-walled carbon nanotubes coated by multi-layer silica for improving thermal conductivity of polymer composites. *J Therm Anal Calorim*. 2013;113: 467–474.
32. Ling YF, Zhang HT, Gu G, Lu XJ, Kayastha V, Jones CS, Shih WS, Janzen DC. A printable CNT-based FM passive wireless sensor tag on a flexible substrate with enhanced sensitivity. *IEEE Sens J*. 2014;14:1193–1197.
33. Prasomsri T, Shi DC, Resasco DE, Anchoring Pd nanoclusters onto pristine and functionalized single-wall carbon nanotubes: a combined DFT and experimental study. *Chem Phys Lett*. 2010;497:103–107.
34. Chen LY, Yu SZ, Wang H, Xu J, Liu CC, Chong WH, Chen HY, General methodology of using oil-in-water and water-in-oil emulsions for coiling nanofilaments. *J Am Chem Soc*. 2013;135: 835−843.
35. Zhang LY, Wan CY, Zhang Y. Morphology and electrical properties of polyamide 6/polypropylene/multi-walled carbon nanotubes composites. *Compos Sci Technol*. 2009;69:2212–2217.
36. Wu J, Xiang FM, Han L, Huang T, Wang Y, Peng Y, Wu HY. Effects of carbon nanotubes on glass transition and crystallization behaviors in immiscible polystyrene/polypropylene blends. *Polym Eng Sci*. 2011;51:585–591.
37. Pötschke P, Bhattacharyya AR, Janke A. Morphology and electrical resistivity of melt mixed blends of polyethylene and carbon nanotube filled polycarbonate. *Polymer*. 2003;44:8061–8069.
38. Zou H, Wang K, Zhang Q, Fu Q. A change of phase morphology in poly(p-phenylene sulfide)/polyamide 66 blends induced by adding multi-walled carbon nanotubes. *Polymer*. 2006;47:7821–7826.
39. Khare RA, Bhattacharyya AR, Kulkarni AR, Saroop M, Biswas A. Influence of multiwall carbon nanotubes on morphology and electrical conductivity of PP/ABS blends. *J Polym Sci B: Polym Phys*. 2008;46:2286–2295.
40. Su C, Xu LH, Zhang C, Zhu J. Selective location and conductive network formation of multiwalled carbon nanotubes in polycarbonate/poly (vinylidene fluoride) blends. *Compos Sci Technol*. 2011;71: 1016–1021.
41. Wu DF, Zhang YS, Zhang M, Yu W. Selective localization of multiwalled carbon nanotubes in poly (ε-caprolactone)/polylactide blend. *Biomacromolecules*. 2009;10:417–424.
42. Göldel A, Kasaliwal G, Pötschke P. Selective localization and migration of multiwalled carbon nanotubes in blends of polycarbonate and poly (styrene-acrylonitrile). *Macromol Rapid Commun*. 2009; 30:423–429.
43. Cayla A, Campagne C, Rochery M, Devaux E. Electrical, rheological properties and morphologies of biphasic blends filled with carbon nanotubes in one of the two phases. *Syn Metals*. 2001;16:1034–1042.
44. Ko SW, Hong MK, Park BJ, Gupta RK, Choi HJ, Bhattacharya SN. Morphological and rheological characterization of multi-walled carbon nanotube/PLA/PBAT blend nanocomposites. *Polym Bull*. 2009; 63:125–134.
45. Xu ZH, Zhang YQ, Wang ZG, Sun N, Li H. Enhancement of electrical conductivity by changing phase morphology for composites consisting of polylactide and poly(ε-caprolactone) filled with acid-oxidized multiwalled carbon nanotubes. *ACS Appl Mater Interfaces*. 2011;3:4858–4864.
46. Baudouin AC, Devaux J, Bailly C. Localization of carbon nanotubes at the interface in blends of polyamide and ethylene–acrylate copolymer. *Polymer*. 2010;51:1341–1354.
47. Khare RA, Bhattacharyya AR, Panwar AS, Bose S, Kulkarni AR. Dispersion of multiwall carbon nanotubes in blends of polypropylene and acrylonitrile butadiene styrene. *Polym Eng Sci*. 2011;51:1891–1905.
48. Li YJ, Shimizu HS. Conductive PVDF/PA6/CNTs nanocomposites fabricated by dual formation of cocontinuous and nanodispersion structures. *Macromolecules*. 2008;41:5339–5344.
49. Göldel A, Marmur A, Kasaliwal GR, Pötschke P, Heinrich G. Shape-dependent localization of carbon nanotubes and carbon black in an immiscible polymer blend during melt mixing. *Macromolecules*. 2011;44:6094–6102.

50. Castillo FY, Socher R, Krause B, Headrich R, Grady BP, Prada-Silvy R, Pötschke P. Electrical, mechanical, and glass transition behavior of polycarbonate-based nanocomposites with different multi-walled carbon nanotubes. *Polymer*. 2011;52:3835–3845.
51. Guo JX, Liu YJ, Prada-Silvy R, Tan YQ, Azad S, Krause B, Pötschke P, Grady BP. Aspect ratio effects of multi-walled carbon nanotubes on electrical, mechanical, and thermal properties of polycarbonate/MWCNT composites. *J Polym Sci Part B: Polym Phys*. 2014;52:73–83.
52. Tchoul MN, Ford WT, Lolli G, Resasco DE, Arepalli S. Effect of mild nitric acid oxidation on dispersability, size, and structure of single-walled carbon nanotubes. *Chem Mater*. 2007;19:5765–5772.
53. Ton-That C, Shard AG, Daley R, Bradley RH. Effects of annealing on the surface composition and morphology of PS/PMMA blend. *Macromolecules*. 2000;33:8453–8459.
54. Kressler J, Higashida N, Inoue T, Heckmann W, Seitz F. Study of polymer-polymer interfaces: a comparison of ellipsometric and TEM data of PMMA/polystyrene and PMMA/SAN systems. *Macromolecules*. 1993;26:2090–2094.
55. Katzen D, Reich S. Image analysis of phase separation in polymers blends. *Europhys Lett*. 1993;21:55–60.
56. Bhattacharyya AR, Ghosh AK, Misra A. Reactively compatibilised polymer blends: a case study on PA6/EVA blend system. *Polymer*. 2001;42:9143–9154.
57. Krause B, Boldt R, Pötschke P. A method for determination of length distributions of multiwalled carbon nanotubes before and after melt processing. *Carbon*. 2011;49: 1243–1247.
58. Kasaliwal GR, Pegel S, Göldel A, Pötschke P, Heinrich G, Analysis of agglomerate dispersion mechanisms of multiwalled carbon nanotubes during melt mixing in polycarbonate. *Polymer*. 2010;51: 2708–2720.
59. Pötschke P, Villmow T, Krause B, Melt mixed PCL/MWCNT composites prepared at different rotation speeds: Characterization of rheological, thermal, and electrical properties, molecular weight, MWCNT macrodispersion, and MWCNT length distribution. *Polymer*. 2013;54:3071–3078.
60. Socher R, Krause B, Müller MT, Boldt R, Pötschke P, The influence of matrix viscosity on MWCNT dispersion and electrical properties in different thermoplastic nanocomposites. *Polymer*. 2012;53: 495–504.
61. Alig I, Pötschke P, Lellinger D, Skipa T, Pegel S, Kasaliwal GR, Villmow T, Establishment, morphology and properties of carbon nanotube networks in polymer melts. *Polymer*. 2012;53:4–28.
62. Tao FF, Nysten B, Baudouin AC, Thomassin JM, Vuluga D, Detrembleur C, Bailly C. Influence of nanoparticle–polymer interactions on the apparent migration behaviour of carbon nanotubes in an immiscible polymer blend. *Polymer*. 2011;52:4798–4805.
63. Nayak GCh, Sahoo S, Rajasekar R, Das CK. Novel approach for the selective dispersion of MWCNTs in the nylon/SAN blend system. *Composite A*. 2012;43:1242–1251.
64. Gültner M, Göldel A, Pötschke P. Tuning the localization of functionalized MWCNTs in SAN/PC blends by a reactive component. *Compos Sci Technol*. 2011;72:41–48.
65. Du B, Handge UA, Maieed S, Abetz V, Localization of functionalized MWCNT in SAN/PPE blends and their influence on rheological properties. *Polymer*. 2012;53:5491–5501.
66. Khan U, Blighe FM, Coleman JN. Selective mechanical reinforcement of thermoplastic polyurethane by targeted insertion of functionalized SWCNTs. *J Phys Chem C*. 2010;114:11401–11408.

Manuscript received Apr. 4, 2014, and revision received Feb. 28, 2015.